Journal of Biomolecular NMR (2006) 35: 241–248
DOI 10.1007/s10858-006-9040-y

Article

Solid state NMR at high magic angle spinning frequencies: Dipolar chemical shift correlation with adiabatic inversion pulse based RF pulse schemes

Christian Herbst, Kerstin Riedel, Jörg Leppert, Oliver Ohlenschläger, Matthias Görlach & Ramadurai Ramachandran*

Molecular Biophysics/NMR spectroscopy group, Leibniz Institute for Age Research, Fritz Lipmann Institute, D-07745, Jena, Germany

Received 2 February 2006; Accepted 30 May 2006

Key words: adiabatic pulse, chemical shift correlation, MAS, solid state NMR

Abstract

The efficacy of hetero- and homonuclear dipolar recoupling employing tanh/tan adiabatic inversion pulse based RF pulse schemes has been examined at high magic angle spinning (MAS) frequencies via numerical simulations and experimental measurements. An approach for minimising the recoupling RF power level is presented, taking into consideration the spinning speed, the range of resonance offsets and H_1 inhomogeneities and the available RF field strength. This involves the tailoring of the frequency and amplitude modulation profiles of the inversion pulses. The applicability of tanh/tan pulse based dipolar recoupling schemes to spinning speed regimes where the performance with conventional rectangular pulses may not be satisfactory is demonstrated.

Introduction

Magic angle spinning (MAS) solid state NMR spectroscopy is a potential alternative tool for the structural investigations of biomolecular systems where the solution state NMR approach is difficult to employ, e.g., due to limited solubility and/or broad spectral lines, or where X-ray diffraction techniques pose difficulties, e.g., in obtaining the required single crystal samples. Although weak homo- and heteronuclear dipolar couplings between low gamma nuclei are generally lost under MAS, a variety of dipolar recoupling procedures have been developed for inhibiting the spatial averaging of these couplings (Bennett et al., 1994; Griffin, 1998; Dusold and Sebald, 2000). This opened up a route for achieving NMR resonance assignments and for the extraction of structural constraints, e.g., internuclear distances and torsion angles, employing isotopically labelled powder specimens. This, in turn, laid the foundation for MAS solid state NMR based structural studies. With a view to provide a general theoretical framework for the design of dipolar recoupling and decoupling sequences, Levitt and co-workers have proposed a symmetry-based approach for effecting the evolution of the spins under the desired average Hamiltonian of interest (Carravetta et al., 2000; Brinkmann and Levitt, 2001; Levitt, 2002). This makes use of the rotational properties of the nuclear spin interactions and involves the application of rotor-synchronised RF pulse sequences. Two classes of symmetry-based pulse sequences, denoted as CN_n^v and RN_n^v have been introduced till date. The CN_n^v class of RF pulse schemes involves the repeated application of a basic element "C" corresponding to an RF cycle with unity propagator $U_{RF}(\tau_C) = \pm 1$. N such cycles are applied over n rotor periods τ_r. Successive C elements are incremented in

*To whom correspondence should be addressed. E-mail: raman@fli-leibniz.de

phase by $\nu 2\pi/N$ and typically the complete CN_n^ν sequence is repeated many times. In the RN_n^ν scheme, the basic component is an inversion element "*R*". A pair of appropriately phase-shifted pulses are derived from this basic element to form a RF pulse sandwich "**R**" and this pulse sandwich is repeated $N/2$ times over n rotor periods so as to form an RF cycle with unity propagator $U_{RF}(\tau_c) = \pm 1$. N, n and ν are all integers and appropriate values for these are chosen, via the selection rule for CN_n^ν and RN_n^ν symmetry, to generate the desired average Hamiltonian with high efficiency. Symmetry-based RF pulse sequences have found extensive usage in MAS NMR studies of biological systems and are typically executed using rectangular RF pulses. One of the difficulties of the symmetry-based RF pulse schemes involving rectangular pulses is that the RF field strength required is related to the spinning speed employed. For example, for CN_n^ν sequences the RF field strength relates to the spinning frequency as $(\omega_1/\omega_r) = (N/n)(\tau_c/\tau_{2\pi})$, where τ_c and $\tau_{2\pi}$ represent the length of the C element and a 2π pulse, respectively. This can result in low recoupling RF field strength requirements and, hence, lead to unsatisfactory performance. Moreover, the efficacy of pulse sequences employing conventional rectangular RF pulses can be sensitive to the RF field strength employed and this may lead to degradation in performance in the presence of RF field inhomogeneities. Recent studies (Heise et al., 2002; Leppert et al., 2002, 2003, 2004; Hardy et al., 2003; Riedel et al., 2004a, b, 2005) indicate that such difficulties can be resolved by implementing RF pulse schemes employing adiabatic inversion pulses.

Since adiabatic pulses were successfully employed in other areas of magnetic resonance to overcome the deleterious effects of H_1 inhomogeneities and resonance offsets (Garwood and DelaBarre, 2001), the primary objective of many of our recent investigations has been to ascertain whether it is equally possible to exploit the potential of adiabatic pulses in MAS solid state NMR. These studies, typically carried out at low or moderate spinning speeds, clearly reveal that the different adiabatic amplitude and frequency modulation profiles already reported in the literature (Garwood and DelaBarre, 2001) can be used for dipolar recoupling/decoupling. Tanh/tan pulses constructed from the following adiabatic half passage and its time reversed half passage,

$$\omega_1(t) = \omega_{1(\max)}\tanh(\xi 2t/T_p)$$

$$\Delta\omega(t) = \Delta\omega_{\max}[\tan(\kappa(1 - 2t/T_p))]/\tan(\kappa),$$

with $\xi = 10$, $\tan(\kappa) = 20$ and $0 \le t \le T_p/2$, as originally reported (Hwang et al., 1998), have found extensive usage. Adiabatic inversion pulse based RF pulse schemes have been reported for MAS solid state NMR studies at high magic angle spinning frequencies (Hardy et al., 2003; Riedel 2004c). Experiments carried out at high spinning speeds offer potentially many advantages, e.g., improved signal to noise ratio. However, the RF power requirements for obtaining satisfactory response from adiabatic pulse schemes could become substantially large where inversion pulses of short durations are required, as typically is the case at high spinning speeds, and render their experimental implementation difficult due to hardware limitations. In this context, we have examined at high MAS frequencies the efficacy of CN_n^ν symmetry-based sequences (Chan and Eckert, 2001; Riedel et al., 2005) for ^{13}C—^{15}N dipolar recoupling/chemical shift correlation employing basic C elements constructed with optimised tanh/tan inversion pulses. The inversion characteristics of the tanh/tan pulses were tailored to a given experimental situation by optimising the parameters ξ, κ and $\Delta\omega_{\max}$ (Tesiram and Robin Bendall, 2002). Additionally, employing tanh/tan adiabatic pulses, we have also evaluated the performance characteristics of the RN_n^ν symmetry-based zero-quantum (ZQ) dipolar recoupling scheme $R6_6^2R6_6^{-2}$ (Brinkmann et al., 2002) for obtaining ^{13}C chemical shift correlation data.

Numerical and experimental procedures

Basic C elements were constructed by suitable concatenation of $180°_x$ and $180°_{-x}$ tanh/tan pulses, e.g., $\{x\bar{x}\}$, $\{xx\bar{x}\bar{x}\}$ and $\{xx\bar{x}\bar{x}\bar{x}\bar{x}xx\}$. The frequency and amplitude modulation profiles of the inversion pulses were tailored so as to obtain satisfactory performance of CN_n^ν symmetry-based RF pulse schemes at the required RF field strength ($\omega_{1(\max)}$) and over the expected range of resonance offsets and H_1 inhomogeneities. This was achieved by first fixing the duration of the tanh/tan pulse, as dictated by N, n, τ_c and τ_r values, and then finding optimal values for the parameters ξ, κ and $\Delta\omega_{\max}$. Numerical

optimisation was carried out via the simulated annealing approach (Kirkpatrick et al., 1983; Sunitha Bai et al., 1993) to obtain either an optimised inversion pulse or a C element directly. The tanh/tan inversion pulse was divided into "**N**" intervals of equal duration ($\sim$0.2 μs) with each element characterised by an amplitude and a phase value $\{a(t),\ \phi(t)\}_{I\,=\,1\ldots N}$. Considering a single spin-1/2 system and neglecting the effects of CSAs, the net propagator, U_{net}, corresponding to either an inversion pulse or the desired basic element C, e.g., $\{xx\overline{x}\overline{x}\}$, was first calculated. The density matrix $\rho(t)$ following this evolution operator, U_{net}, was then obtained, starting from an initial state $\rho(0)$ of I_z. The error function $\varepsilon(\xi, \kappa, \Delta\omega_{max})$ representing the deviation of the density matrix $\rho(t)$ from the required ρ(ideal) was calculated over a 2D grid of resonance offsets and H_1 field strength. The maximum value ε_{max} seen in the 2D error surface was always employed in our simulated annealing approach for scanning the configuration space, i.e., ξ, κ and $\Delta\omega_{max}$, in order to find optimal values. A sufficiently slow cooling schedule was applied and the temperature/control parameter of the simulated annealing protocol was altered after either 100 successful uphill moves or 1000 attempted uphill moves. R (representing the product of the pulsewidth and $\Delta\omega_{max}$), ξ and tanκ were varied over a range of 10–150, 0–100 and 0–100, respectively, for generating optimised inversion pulses/basic C elements. The simulated annealing procedure was terminated when there was no significant difference in ε_{max} between two successive temperature changes.

As in our recent study (Riedel et al., 2005), the performance characteristics of different ^{13}C—^{15}N dipolar recoupling sequences were evaluated numerically via the transferred echo double resonance (TEDOR) technique (Hing et al., 1992). TEDOR is commonly employed for obtaining ^{13}C—^{15}N dipolar chemical shift correlation spectra, both in the context of resonance assignments and for the simultaneous measurement of multiple carbon–nitrogen distances, in uniformly $\{^{13}C, ^{15}N\}$ labelled samples (Jaroniec et al., 2002). Simulations were carried out considering two spin-1/2 heteronuclei ($I-S$) and the magnitude of the I spin (^{13}C) magnetisation observed at $t_2 = 0$ was monitored as a function of the net heteronuclear dipolar recoupling period (τ_m).

The efficacy of RN_n^ν symmetry-based zero-quantum (ZQ) dipolar recoupling scheme (Brinkmann et al., 2002) with tanh/tan adiabatic pulses was assessed by monitoring the z magnetisation transferred to the second spin ($^{13}C'/^{13}C^{\beta}$) as a function of the mixing time, starting with z magnetisation on spin 1 ($^{13}C^{\alpha}$). Unless mentioned otherwise, ^{13}C scalar coupling, chemical shift and dipolar tensor parameters of alanine ($C^{\alpha} \rightarrow C^{\beta}$) and glycine ($C^{\alpha} \rightarrow C'$) were employed in these simulations (Brinkmann et al., 2002; Leppert et al., 2003). Simulations were carried out using the SIMPSON program (Bak et al., 2000), at a Zeeman field strength of 11.7 T and for representative spinning speeds as indicated in the figure captions. Experiments were carried out with undiluted $\{^{15}N, ^{13}C\}$ labelled samples of histidine at room temperature on a 500 MHz wide-bore Varian ^{UNITY}INOVA solid state NMR spectrometer equipped with a 3.2 mm Chemagnetics triple resonance probe and waveform generators for pulse shaping. The frequency sweep is implemented in the spectrometer hardware as a phase modulation, $\phi(t) = \int\Delta\omega(t)dt$. Cross-polarisation under Hartmann–Hahn matching conditions was employed and all spectra were collected under high power ^1H decoupling. The RF pulse sequences employed for generating hetero- and homonuclear chemical shift correlation spectra were similar to those used in our recent studies (Riedel et al., 2004b, 2005; Leppert et al., 2003).

Results and discussion

Contour plots of the observed I_z magnetisation, as a function of RF field strength and resonance offset, after the application of inversion pulses of duration 25 μs and basic C elements ($\{xx\overline{x}\overline{x}\}$, 100 μs) indicated in the figure caption are given in Figure 1. These plots were generated considering a single spin-1/2 system and neglecting CSA. The plot for a tanh/tan inversion pulse characterised by R, tanκ and ξ values of 60, 20 and 10, respectively, and as employed in our recent studies (Leppert et al., 2003; Riedel et al., 2004b, 2005), is shown in Figure 1a. It is seen that for obtaining satisfactory performance, even over a small resonance offset range of $\pm$10 kHz, an RF field strength in the range of $\sim$50 kHz will be required. Although the

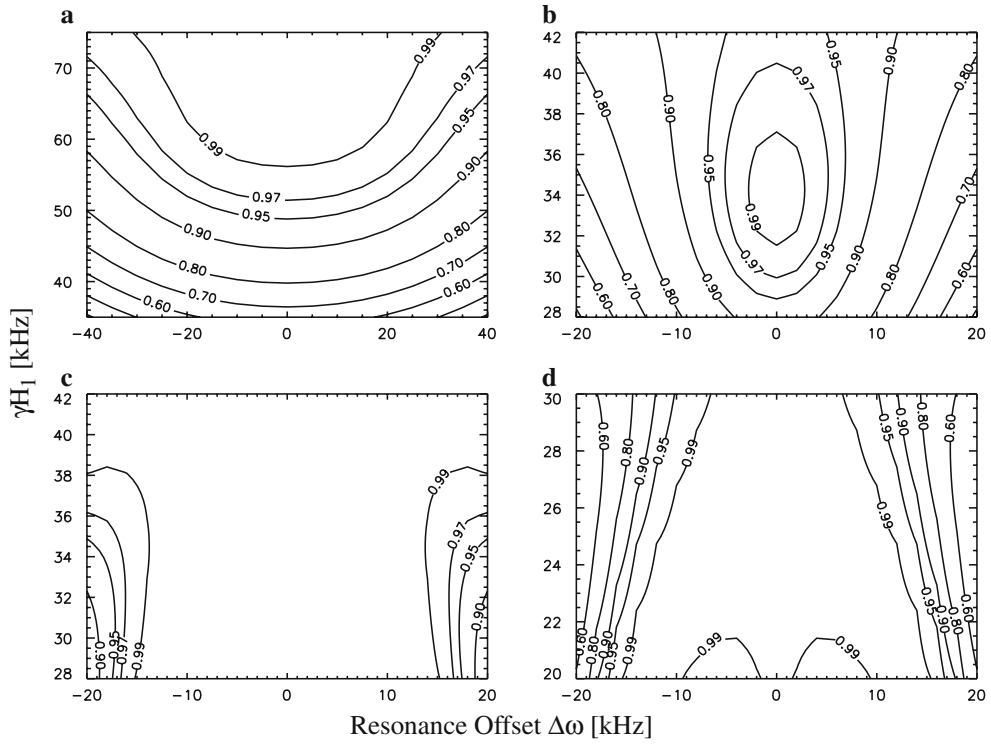

Figure 1. Contour plots of $< -I_z >$ (a and b) and $< I_z >$ magnetisation (c and d) (expressed as a fraction of the initial magnetisation and as a function of the RF field strength and resonance offset) after the application of either an inversion pulse or the basic *C* element $\{xx\overline{x}\overline{x}\}$ constructed employing tanh/tan adiabatic pulses. The plots were obtained with tanh/tan inversion pulses characterised, respectively, by R, tanκ and ξ values of 60, 20 and 10 (a) and 25.3, 18.4 and 91.25 (b). Plots c and d were generated with *C* elements constructed with adiabatic pulses defined by R, tanκ and ξ values of 25.3, 18.4 and 91.25 (c) and 15.57, 15.57 and 89.53 (d).

RF power requirements can be reduced with inversion pulses of longer durations (Leppert et al., 2002), pulses with short durations are often needed. For example, to achieve $^{13}C—^{15}N$ heteronuclear dipolar recoupling at a spinning speed of 20 kHz and with the $C2_4^1$ symmetry-based sequence (Riedel et al., 2005) employing the *C* element $\{xx\overline{x}\overline{x}\}$ would require inversion pulses of durations of 25 μs. In situations where high ^{15}N RF field strengths are not available, e.g., as typically is the case with MAS NMR probes with large rotor diameters, and for minimising the interference between the recoupling and decoupling RF irradiations, it will be advantageous to have inversion pulses that perform satisfactorily at low RF power levels. Considering a ^{15}N chemical shift dispersion of ~300 ppm and ±10% variation in the RF field strength due to H_1 inhomogeneities, we have constructed optimised inversion pulses and basic *C* elements. The plot for the optimised inversion pulse characterised by R, tanκ and ξ values of 25.3, 18.4 and 91.25, respectively, and generated for satisfactory performance with an RF field strength of 35 kHz and over a ±10 kHz range of resonance offsets is given in Figure 1b and the plot for the *C* element derived from this optimised pulse is shown in Figure 1c. Although the inversion pulse does not exhibit 100% inversion over the desired range of resonance offsets and H_1 inhomogeneities, the phase cycling used in the construction of the *C* element, as expected, leads to significantly improved performance. Figure 1d shows the plot for a *C* element optimised directly, for satisfactory performance with an RF field strength of 25 kHz and over a resonance offset range of ±10 kHz. Tanh/tan pulses characterised by R, tanκ and ξ values of 15.57, 15.57 and 89.53, respectively, were employed in the *C* element. These plots suggest that it is possible, in principle, to minimise the RF power level requirements of tanh/tan pulses by tailoring the amplitude and frequency modulation profiles.

The efficacy of heteronuclear dipolar recoupling with optimised tanh/tan inversion pulses were first assessed via numerical simulations. Simulated TEDOR transfer characteristics for a spinning speed of 20 kHz and as a function of the ^{15}N RF field strength and resonance offset are given in Figure 2a–f. As in our earlier study (Riedel et al., 2005), to assess the relative merits of different pulse schemes clearly, a weak ^{13}C—^{15}N dipolar coupling strength of 190 Hz was employed in these simulations. From our earlier studies (Riedel et al., 2005), the effects of ^{15}N CSAs on the TEDOR performance were found to be negligible, even at a spinning speed of 10 kHz. Hence these were neglected in the simulations shown here. Except for the ^{15}N pulses applied during the dipolar recoupling periods, all RF pulses were assumed to be δ pulses in the numerical calculations. Plots obtained with $C2_4^1$ symmetry-based RF pulse scheme with the *C* element $\{xx\overline{xx}\}$ based on tanh/tan pulses and designed for satisfactory performance at RF field strengths of 35, 30 and 25 kHz, respectively, are given in Figure 2a–c. For comparison, the simulated TEDOR plots obtained with $C2_4^1$ pulse scheme with tanh/tan pulses having, respectively, R, tanκ and ξ values of 60, 20 and 10 (Figure 2d), $C3_3^1$ pulse scheme employing the POST *C* element $\{(\pi/2)_0(2\pi)_\pi(3\pi/2)_0\}$ with rectangular RF pulses (Chan and Eckert, 2001) (Figure 2e) and conventional dipolar recoupling with rectangular ^{15}N inversion pulses (20 μs) applied at the middle and end of the rotor period and with xy-8 phasing scheme (Gullion et al., 1990) (Figure 2f) are also given. Figure 2d shows that it is possible to obtain with tanh/tan pulses characterised by R, tanκ and ξ values of 60, 20 and 10, respectively, good TEDOR performance employing an RF field strength of ~50 kHz. However, satisfactory performance at lower RF power levels can be obtained by optimising the amplitude and frequency modulation functions (Figure 2a–c). It is also seen that the TEDOR transfer characteristics with ^{15}N irradia-

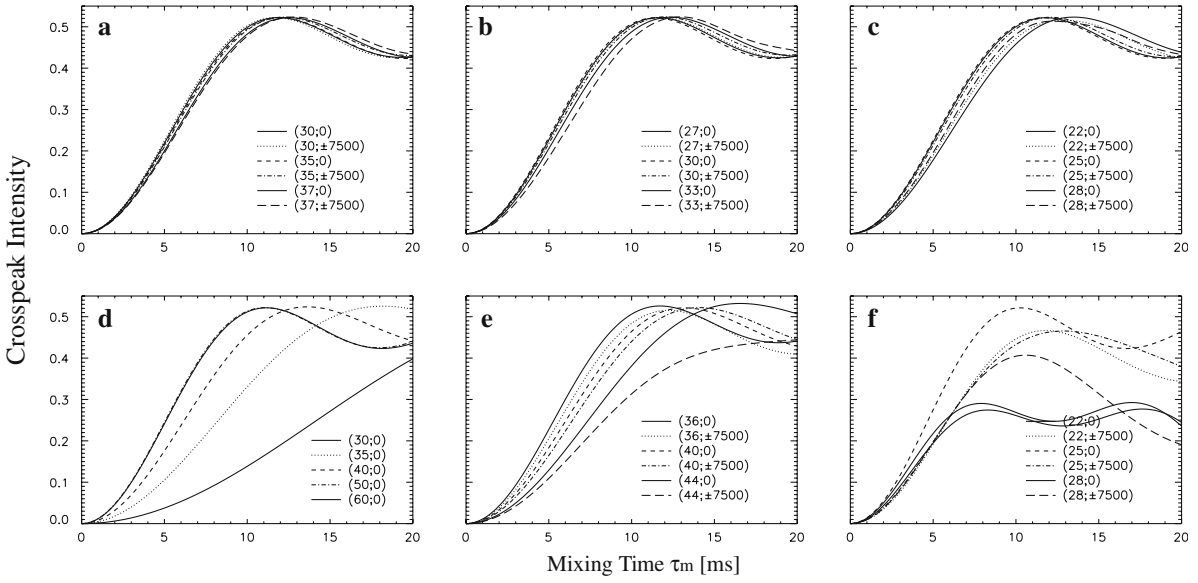

Figure 2. Simulated TEDOR plots generated at a spinning speed of 20 kHz and as a function of the RF field strength and resonance offset for ^{15}N RF irradiation. All simulations were carried out employing a ^{13}C—^{15}N dipolar coupling strength of 190 Hz and neglecting ^{15}N CSAs. The RF field strength (kHz) and the resonance offsets (Hz) employed in the simulations are indicated, respectively, by the two numbers shown corresponding to each of the plots. The sampled data points were interpolated to provide visual clarity. Euler angles defining the orientation of CS tensors in an arbitrary molecular frame were fixed at (0°, 0°, 0°) and the orientation of the dipolar vector in the molecular frame was fixed at (0°, 0°). Plots a, b, c and d were obtained with tanh/tan pulses characterised by R, tanκ and ξ values of (25.3, 18.4, 91.25), (68.2, 62.9, 96.9), (15.57, 15.57, 89.53) and (60, 20, 10), respectively, employing the $C2_4^1$ symmetry-based adiabatic heteronuclear dipolar recoupling scheme with the basic *C* element $\{xx\overline{xx}\}$. Results for the $C3_3^1$ symmetry-based dipolar recoupling scheme employing the POST *C* element $\{(\pi/2)_0(2\pi)_\pi(3\pi/2)_0\}$ with rectangular RF pulses and that for conventional dipolar recoupling with rectangular ^{15}N inversion pulses (20 μs) applied at the middle and end of the rotor period and with xy-8 phasing scheme are given, respectively, in e and f.

tion schemes employing conventional 20 μs rectangular RF pulses are far from satisfactory (Figure 2f). Numerical simulations indicate that the reduction in the RF power level requirements with optimised tanh/tan pulses has been achieved without sacrificing the sensitivity of the initial rate of build up of the I spin intensities to the heteronuclear dipolar coupling strength and hence to the internuclear distance involved (data not shown). Employing RF field strengths of the order of 30–35 kHz, these results clearly show that it is possible to extend the applicability of TEDOR with optimised tanh/tan pulses to spinning speeds higher than what was demonstrated earlier (Riedel et al., 2005).

The performance of RN_n^ν ZQ homonuclear dipolar recoupling scheme $R6_6^2R6_6^{-2}$ with the composite pulse inversion element R $[90_{180}270_0]$ (Brinkmann et al. (2002)) (Figure 3a and c) and tanh/tan adiabatic pulses (Figure 3b and d) was assessed at a spinning speed of 25 kHz. Tanh/tan pulses of 40 μs durations and having, respectively, R, tanκ and ξ values of 60, 20 and 10 were used. Considering that the recoupling RF field strength needed with the composite pulse R element is related to the spinning speed (Brinkmann et al., 2002) and the RF field strength required with adiabatic pulses is dependent only on the pulse characteristics, simulations were carried out at RF field strengths indicated. Figure 3 shows that improved ZQ dipolar recoupling can be achieved by employing the tanh/tan adiabatic inversion element R. ^{13}C RF field strengths of the order of 40–50 kHz are typically available even in 5 mm MAS NMR probes. Considering that satisfactory performance can be obtained with tanh/tan pulses having, respectively, R, tanκ and ξ values of 60, 20 and 10, we have not attempted to reduce the RF power requirements by tailoring the tanh/tan pulse characteristics.

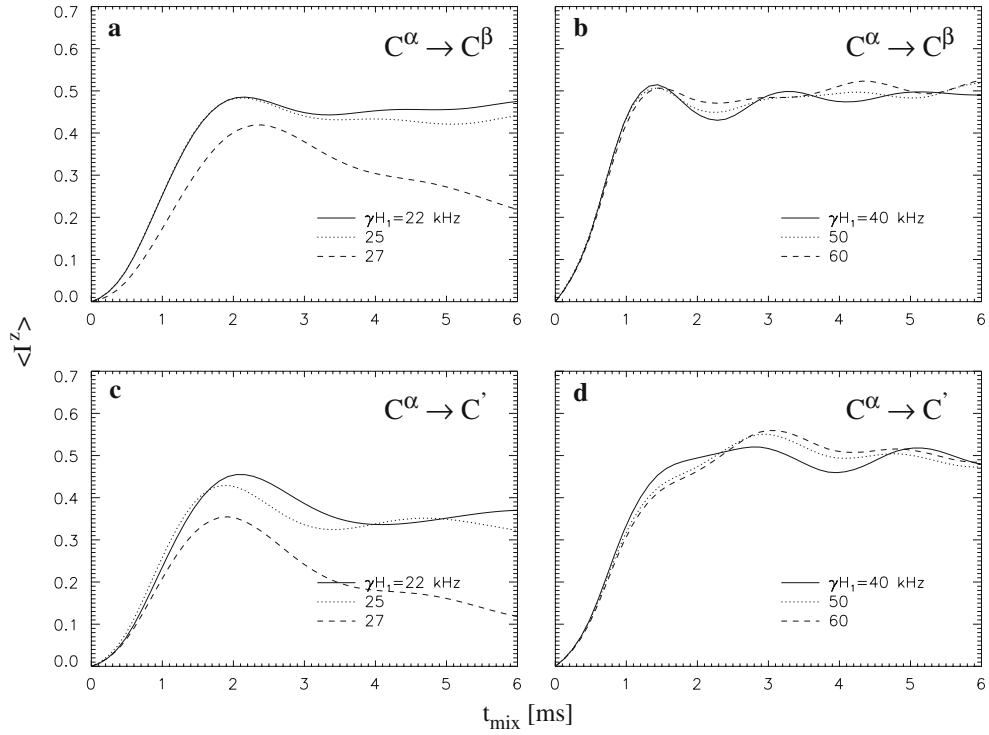

Figure 3. Magnitude of the transferred magnetisation on spin 2 ($^{13}C^\beta/^{13}C'$) (normalised to the maximum transferable signal) as a function of the RF field strength employed and starting with longitudinal magnetisation on spin 1 ($^{13}C^\alpha$) at zero mixing time. Plots at the spinning speed of 25000 Hz and with the ZQ dipolar recoupling scheme $R6_6^2R6_6^{-2}$ were obtained using the composite pulse R element $[90_{180}270_0]$ (a and c) and tanh/tan pulses of 40 μs duration and defined by R, tanκ and ξ values of (60, 20, 10) (b and d). The sampled data points were interpolated to provide visual clarity. Simulations were carried out employing ^{13}C CS tensor, scalar, dipolar coupling and other parameters of alanine and glycine as in earlier studies (Leppert et al., 2003; Riedel et al., 2004b). The ^{13}C RF carrier was kept at 110 ppm in these simulations.

To confirm the applicability of adiabatic hetero- and homonuclear dipolar recoupling RF pulse schemes at high magic angle spinning frequencies, we have performed $^{13}C—^{15}N$ and $^{13}C—^{13}C$ dipolar chemical shift correlation experiments on a model system, an uniformly $\{^{15}N, ^{13}C\}$ labelled polycrystalline sample of histidine. The heteronuclear correlation spectrum obtained employing the TEDOR sequence (Riedel et al., 2005) is given in Figure 4. It was generated at a spinning speed of 20 kHz, with a short mixing time of 1.6 ms, using $C2_4^1$ symmetry-based dipolar recoupling scheme with basic *C* element $\{xx\overline{x}\overline{x}\}$ constructed with optimised tanh/tan adiabatic pulses of 25 μs durations and employing an RF field strength of ~28 kHz. Other details are given in the figure caption. All the expected cross peaks arising from short range (one-bond) heteronuclear dipolar interactions are clearly seen in the spectrum. The homonuclear ^{13}C chemical shift correlation spectrum generated with the $R6_6^2R6_6^{-2}$ dipolar recoupling scheme using tanh/tan pulses of 40 μs durations, an RF field strength of ~40 kHz, mixing time of 3.8 ms and a spinning speed of 25 kHz is given in Figure 5. As expected, crosspeaks arising from relayed magnetisation transfers, besides one-bond correlation peaks, are also seen. To minimise the interference between the recoupling and decoupling RF fields, it is advantageous to carry out these experiments with maximum difference between the recoupling and decoupling RF field strengths, typically > 1:3. Our current studies were carried out with ^1H decoupling field strength of ~125 kHz. In this context, it is worth pointing out that recently progress has been made in designing recoupling schemes that can be ap-

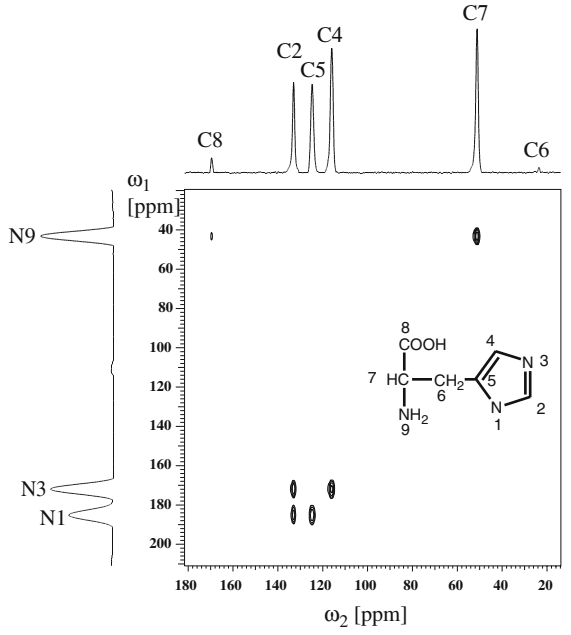

Figure 4. $^{13}C—^{15}N$ dipolar chemical shift correlation spectrum of histidine (zoomed plot) collected at a spinning speed of 20 kHz, 32 t_1 increments, 10 kHz spectral width in ω_1, 32 scans per t_1 increment, 5 s recycle time and with a heteronuclear dipolar recoupling period of 1.6 ms, $C2_4^1$ symmetry-based dipolar recoupling scheme with basic *C* element $\{xx\overline{x}\overline{x}\}$ based on optimised tanh/tan adiabatic pulses of 25 μs durations and defined by R, tanκ and ξ values of (15.57, 15.57 and 89.53) and with an RF field strength of ~28 kHz.

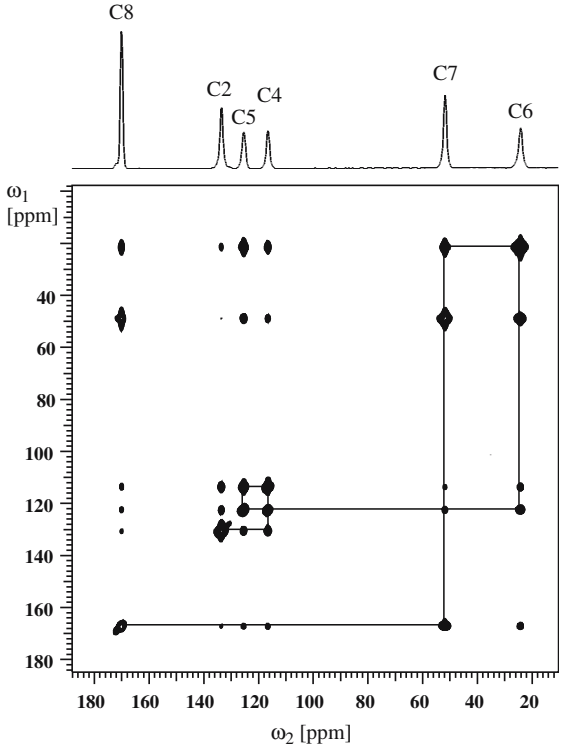

Figure 5. Experimental ^{13}C ZQ correlation spectrum (zoomed plot) of histidine obtained at a spinning speed of 25 kHz and with adiabatic symmetry-based $R6_6^2R6_6^{-2}$ scheme. The spectrum was obtained with a recycle time of 5 s, 16 scans per t_1 increment, ω_1 spectral width of 50000 Hz, a dipolar mixing time of 3.84 ms, tanh/tan adiabatic inversion pulses of 40 μs duration and defined by R, tanκ and ξ values of (60, 20, 10) and with $\omega_{1(max)}/2\pi$ of ~40 kHz.

plied without ^{1}H decoupling. For example, using a ^{13}C RF field strength of 100 kHz, broadband ^{13}C chemical shift correlation without ^{1}H decoupling has been demonstrated recently at a spinning speed of 28.6 kHz (De Paepe et al., 2006). However, such high ^{13}C RF field strengths are not typically available in MAS NMR probes of larger diameters. Under these circumstances, it is expected that methods such as that outlined here will be of great value. In conclusion, the data presented here clearly show that it is possible to tailor the frequency and amplitude modulation profiles of the tanh/tan inversion pulses to reduce the RF power requirements, implement efficient tanh/tan inversion pulse based dipolar correlation experiments at high magic angle spinning frequencies and improve the efficacy of symmetry-based dipolar recoupling schemes in the spinning speed regimes where the performance with conventional rectangular pulses may not be satisfactory.

Acknowledgements

This study has been funded in part by a PhD fellowship to Kerstin Riedel from Stiftung Stipendien-Fonds des Verbandes der Chemischen Industrie e.V.

References

Bak, M., Rasmussen, J.T. and Nielsen, N.C. (2000) *J. Magn. Reson.*, **147**, 296–330.

Bennett, A.E., Griffin, R.G. and Vega, S. (1994) *NMR Basic Principles and Progress*, Springer Verlag, Berlin, **33**, 1–77.

Brinkmann, A. and Levitt, M.H. (2001) *J. Chem. Phys.*, **115**, 357–384.

Brinkmann, A., Schmedt auf der Günne, J. and Levitt, M.H. (2002) *J. Magn. Reson.*, **156**, 79–96.

Carravetta, M., Eden, M., Zhao, X., Brinkmann, A. and Levitt, M.H. (2000) *Chem. Phys. Lett.*, **321**, 205–215.

Chan, J.C.C. and Eckert, H. (2001) *J. Chem. Phys.*, **115**, 6095–6105.

Dusold, S. and Sebald, A. (2000) *Annu. Rep. NMR Spectrosc.*, **41**, 185–264.

De Paepe, G., Bayro, M.J., Lewandowski, J. and Griffin, R.G. (2006) *J. Am. Chem. Soc.,* **128**, 1776–1777.

Garwood, M. and DelaBarre, L. (2001) *J. Magn. Reson.*, **153**, 155–177.

Griffin, R.G. (1998) *Nature Struct. Biol.*, **5**, 508–512.

Gullion, T., Baker, D.B. and Conradi, M.S. (1990) *J. Magn. Reson.*, **89**, 479–484.

Hardy, E.H., Detken, A. and Meier, B.H. (2003) *J. Magn. Reson.*, **165**, 208–218.

Heise, B., Leppert, J., Ohlenschläger, O., Görlach, M. and Ramachandran, R. (2002) *J. Biomol. NMR*, **24**, 237–243.

Hing, A.W., Vega, S. and Schaefer, J. (1992) *J. Magn. Reson*, **96**, 205–209.

Hwang, T., van Zijl, P.C.M. and Garwood, M. (1998) *J. Magn. Reson.*, **133**, 200–203.

Jaroniec, C.P., Filip, C. and Griffin, R.G. (2002) *J. Am. Chem. Soc.*, **124**, 10728–10742.

Kirkpatrick, S., Gelatt, C.D. and Vecchi, M.P. (1983) *Science*, **220**, 671–680.

Leppert, J., Heise, B., Görlach, M. and Ramachandran, R. (2002) *J. Biomol. NMR*, **23**, 227–238.

Leppert, J., Heise, B., Ohlenschläger, O., Görlach, M. and Ramachandran, R. (2003) *J. Biomol. NMR*, **26**, 13–24.

Leppert, J., Ohlenschläger, O., Görlach, M. and Ramachandran, R. (2004) *J. Biomol. NMR*, **29**, 167–173.

Levitt, M.H. (2002) *Encyclopedia NMR*, **9**, 165–196.

Riedel, K., Leppert, J., Ohlenschläger, O., Görlach, M. and Ramachandran, R. (2004a) *Chem. Phys. Lett.*, **395**, 356–361.

Riedel, K., Leppert, J., Hafner, S., Ohlenschläger, O., Görlach, M. and Ramachandran, R. (2004b) *J. Biomol. NMR*, **30**, 389–395.

Riedel, K. (2004c) Diploma thesis, Friedrich-Schiller-university, Jena.

Riedel, K., Leppert, J., Ohlenschläger, O., Görlach, M. and Ramachandran, R. (2005) *J. Biomol. NMR*, **31**, 49–57.

Sunitha Bai, N., Ramakrishna, M. and Ramachandran, R. (1993) *J. Magn. Reson. A*, **102**, 235–240.

Tesiram, Y.A. and Robin Bendall, M. (2002) *J. Magn. Reson.*, **156**, 26–40.